Catalytic Pyrogasification of Biomass. Evaluation of Modified Nickel Catalysts

Jesús Arauzo,† Desmond Radlein, Jan Piskorz, and Donald S. Scott*

Department of Chemical Engineering, University of Waterloo, Waterloo, Ontario, Canada N2L 3G1

In a previous work, the pyrolytic gasification of biomass (wood) using a stoichiometric nickel aluminate catalyst in a fluidized-bed reactor gave near-equilibrium yields of products above 650 °C, with 85−90% gas yields and no detectable tar production. Additional tests are reported for a modified nickel−magnesium aluminate stoichiometric catalyst, to give greater physical strength, and for the addition of potassium, as a promoter. The addition of Mg in the catalyst crystal lattice did improve resistance to attrition but resulted in a minor loss in gasification activity and increased coke production. Addition of potassium had little effect. Catalyst deactivation by secondary carbon deposits was demonstrated, and regeneration of the Mg-containing catalysts by burn-off appears to be feasible. The deactivation process was experimentally simulated. A conceptual process for catalytic pyrogasification of biomass was modeled.

Introduction

Gasification of biomass has been extensively studied, and a voluminous journal and patent literature exists. Among the many excellent reviews available, two recent publications may be mentioned as useful references, by Bridgwater and Double (1988) and by Beenackers and Bridgwater (1989). In the great majority of autothermal gasification studies air, oxygen, steam, or mixtures of these have been used as gasifying media. In most developments, no catalysts have been employed. Only in more recent years have reports appeared concerning the effects of catalysts in various pyrolytic biomass gasification schemes.

A distinction must be made between conventional gasification, in which a reactive gas, usually oxygen or steam, is a major factor, and pyrolytic gasification, which does not require any additional reactants, although limited amounts may be used, particularly of steam or carbon dioxide. Pyrolytic gasification is endothermic, and heat must be added from some external source. Extensive studies by workers at Battelle of pyrolytic gasification using catalysts have been described by Mudge et al. (1987), and the catalytic methanation of wood with carbon conversions to methane of over 80% has been described by Garg et al. (1988), to give only two recent examples.

There are two advantages apparent in the use of catalysts for the pyrolytic gasification of biomass. First, the gasification reactions can be made to occur at much lower temperatures and with only small amounts of steam or carbon dioxide, if any, resulting in energy economies as well as the possibility of altering product compositions because of equilibrium relationships. Second, the catalyst, because of the greater reaction rates possible, may give a gas product more nearly at equilibrium yields and thus allow more accurate predictions of product composition to be made.

In some tests with nickel on alumina-supported catalysts, we had observed that, even in an inert gas atmosphere (nitrogen), high gas yields could be obtained in the surprisingly low temperature range of 500−650 °C. A more recent study (Arauzo et al., 1994) carried out using a crystalline nickel aluminate catalyst has shown an effective behavior for biomass catalytic gasification processes at temperatures from 600 to 650 °C. Temperatures of 650 °C or above appeared to be adequate for complete reforming of the tar vapors, and no tar production was observed in either inert or reactive gasification media and without any added oxygen or air. The influence of the nickel catalyst and of operating conditions on the nature of the gasification products was also investigated. Evidence was presented which indicated that the gasification mechanism was a fast thermal pyrolysis followed by catalytic re-forming of the vapors with a high yield of synthesis gas. Gas compositions of 90 vol % (N_2 free) of H_2 plus CO were achieved.

From the practical point of view, the hydrogen which could be produced from a biomass gasification plant of feasible size, say 1000 tons/day, would be adequate for the hydrocracking or hydrotreating of about 15 000−30 000 bbls/day of heavy petroleum refinery residue, tar sand stripped bitumen, or other heavy crudes or residues. This would appear to be one of the few instances in the energy field in which the feasible scale of operation of a biomass conversion plant can be matched to an economical operating level for a petroleum process.

For these reasons and because of the promising results obtained with the crystalline nickel aluminate catalyst, it was decided to undertake more extensive investigations of catalytic gasification of biomass, with two objectives: (i) to improve catalyst characteristics for use in a fluidized-bed reactor with respect to attrition and carbon deposition, and (ii) to study catalyst deactivation and its consequences on tar formation, kinetics, etc.

The present paper describes a part of this study in which modifications of the nickel aluminate, $NiAl_2O_4$, catalyst (addition of Mg and K) and aspects of catalyst deactivation/regeneration were investigated. Finally, a conceptual scheme for a continuous catalytic biomass gasification plant is also described.

Experimental Section

Materials Used. Biomass. All the gasification tests reported were done with a standard hybrid poplar wood obtained from the International Energy Agency. This

* To whom correspondence should be addressed. e-mail: e11541@chemical.uwaterloo.ca.

† Present address: Department of Chemical and Environmental Engineering, University of Zaragoza, 50015 Zaragoza, Spain. e-mail: qtarauzo@cc.unizar.es.

S0888-5885(95)00271-5 CCC: $14.00

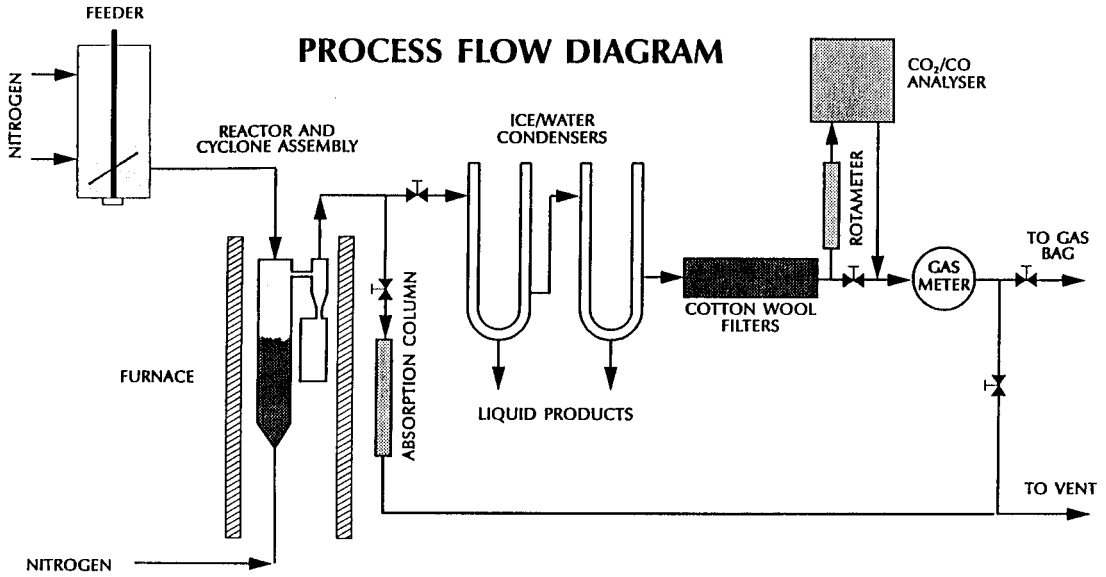

Figure 1. Schematic drawing of a bench-scale gasification unit.

wood was ground and dried to give a feed material with a −0.5 mm particle size and a moisture content between 4.8 and 5.8%. The analysis of this material is given by Scott (1990) is shown below.

extractives	3.0	wt %
lignin	23.5	
hemicellulose	20.0	
cellulose	49.1	
ash	0.46	
	96.1	wt %, dry
other substances, losses, analytical errors	3.9	wt %
	100.0	wt %
elemental analysis		
carbon	50.5	wt %, maf
hydrogen	6.2	
oxygen	43.2	
nitrogen	0.06	
ash	0.46	
higher heating value, maf	4661 cal/g	

Catalysts. Catalysts used in this work are types of modified nickel alumina formulations, and stoichiometric nickel aluminate, $NiAl_2O_4$, has been considered the base material for later modifications. The nickel aluminate is a crystalline stoichiometric compound, green in color, with a spinel lattice structure. It was prepared in-house.

The catalyst modifications can be summarized in two groups, one in which magnesium has replaced some of the nickel in the crystal lattice and a second group in which potassium has been added physically. In the first group, the magnesium substitution was made at two different levels, replacing 25% (molar basis) of the nickel to give a catalyst composition which can be represented as $Ni_3MgAl_8O_{16}$ containing 26% nickel and 3.6% magnesium and replacing 50% of the nickel to give $NiMgAl_4O_8$ with 18.3% nickel and 7.6% magnesium. The magnesium addition was made to increase the physical strength of the catalyst and its resistance to attrition.

Some potassium compounds have been reported as effective promoters for carbon gasification; therefore, several ways to add this cation were tried. In three cases, 2% of KOH was incorporated into the nickel aluminate by different procedures: by wetting the dry nickel catalyst (type a), by impregnation of the catalyst (type b), and by precipitate inclusion (type c). A fourth catalyst was prepared by the latter method but with 8% KOH addition (type d).

The bulk density of all these catalysts is about 1100 kg/m^3 and the particle size used was $-250 + 75$ μm which gave a u_{mf} (minimum fluidization velocity) equal to 0.0121 m/s at room temperature.

The structures of the fresh and used Mg-containing catalysts were determined by BET and mercury intrusion porosimetry. Furthermore, a visual analysis by electron microscopy was made in order to observe possible surface changes. The samples were also characterized by X-ray powder diffraction (XRD) and from these analyses $NiAl_2O_4$ and $MgAl_2O_4$ spinels were clearly observed, but some amorphous forms were also present, probably due to the presence of minor amounts of Al_2O_3 and NiO.

Sand. Ottawa sand with a particle size of 105−149 μm was used for dilution of the catalyst for simulation of catalyst deactivation, together with $NiMgAl_4O_8$ formulation as described above. In several experiments, this mixture of sand and catalyst in variable proportions was used as the fluidized solid.

Apparatus. A process flow diagram of the experimental system is shown in Figure 1. Nitrogen (or for some experiments CO_2) was used to transport the wood particles continuously into the bench-scale fluidized-bed reactor at feed rates of 10−100 g/h. Nitrogen entered the base of the reactor to fluidize the bed of catalyst particles. The process operated at essentially atmospheric pressure. All solid, liquid, and gaseous products were collected, and a material balance was attempted. The concentrations of carbon monoxide and carbon dioxide were continuously monitored as the experiment progressed by an on-line infrared gas analyzer to observe changes in catalyst performance and activity. Actual gas concentrations were determined by GC analysis.

The product recovery system was designed to permit a complete material balance to be obtained since each unit, as well as the connecting lines, could be disassembled and weighed before and after the experiment. The condensers and all the lines were washed with methanol at the conclusion of a run to obtain the "methanol solubles" composed of tar and water.

Table 1. Physical Characteristics of Nickel Catalyst

	run no.[a]							
	113		121		120		122	
	fresh	used	fresh	used	fresh	used	fresh	used
macrointrusion volume (mL/g)	0.543	0.636	0.509	0.294	0.473	0.265	0.518	ND[b]
macropore area (m^2/g)	0.051	0.046	0.042	0.023	0.043	0.022	0.047	ND[b]
median pore diameter − area (μm)	40.4	57.1	46.7	43.7	42.9	41.6	43.8	ND[b]
BET (m^2/g)	154.3	137.3	150.8	129.6	140.4	114.5	160.3	125.04

[a] 113 = nickel aluminate, first batch, $NiAl_2O_4$. 122 = nickel aluminate, second batch. 121 = Mg/Ni mole ratio 0.33, $Ni_3MgAl_8O_{16}$. 120 = Mg/Ni mole ratio 1.0, $NiMgAl_4O_8$. [b] ND = not determined.

Analysis of gases was carried out by chromatography, and water in the condensate was determined by Karl Fischer titration. For some experiments tar analyses were required, and these were carried out by GC−MS.

A detailed description of the methods and procedures used in this "bench-scale" pyrolysis unit as well as of analytical methods has been given by Scott and Piskorz (1982) and Scott et al. (1985).

Product yields are reported as percent by weight of feed on a moisture-free basis. Gas yields are reported as percent by weight of feed.

Results

(a) Effect of Magnesium Addition. Because the stoichiometric nickel aluminate catalyst was not strongly resistant to attrition in the fluidized bed, magnesium was added which is reported to be able to replace nickel in the crystal structure and to add physical strength to the catalyst (Koryabkina et al., 1991; Ovsyannikova et al., 1989). As described earlier, magnesium was substituted for nickel to give mole ratios of Mg/Ni in the catalyst of 0.00, 0.33, and 1.00.

BET and mercury intrusion porosimeter evaluations were done on these catalysts to see if the stronger structure was reflected by important changes in surface area, pore volume, or size. BET surface area was determined from the corresponding isotherm using nitrogen as an adsorbent. Results for fresh and used catalysts are shown in Table 1. The catalyst corresponding to run 113 (no Mg) was made earlier, and since it showed a catalytic activity a little higher than normal, a second measurement was done with a catalyst from a later batch (run 122, no Mg) for comparison.

Results in Table 1 indicate that the substitution of the magnesium for nickel does lead to a reduction of the surface area and to a smaller pore volume, although mean pore diameters are essentially unchanged. The pore size distribution given, obtained by mercury porosimetry, is for sizes above about 8 μm. The bulk of these macropores were in the range of 30−80 μm with an average value of 45 μm. The incremental intrusion volumes as a function of pore diameter are shown in Figure 2 and show the similarity in pore size distribution but reduction in pore volume as the Mg content increases.

Comparison of electron microscope pictures of fresh and used catalyst showed a significant carbon deposition on the surface. This deposit appeared to be very open and porous in nature and did not appear to adversely affect catalyst activity. Comparison of the used catalyst with a deactivated catalyst showed that the carbon deposit had become less porous and appeared somewhat denser.

Gasification tests were carried out for the catalysts designated as runs 113, 121, and 120 in Table 1. All tests used an initial catalyst charge of 50 g and were done at 600 °C. The results are given in Table 2.

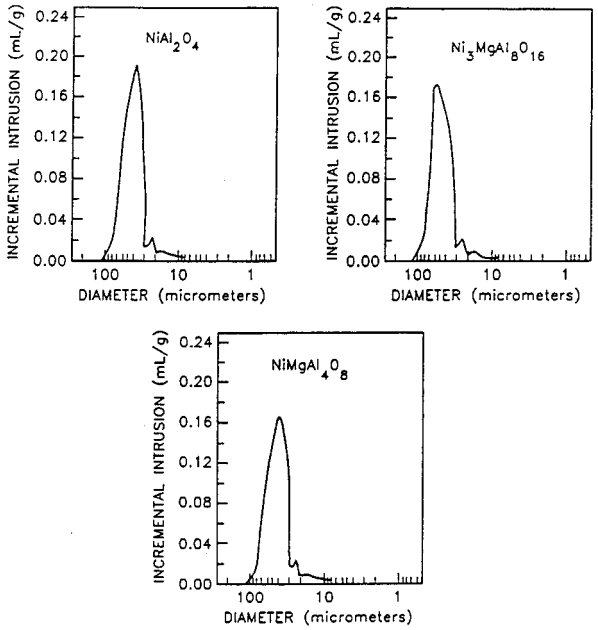

Figure 2. Mercury porosimetry incremental volume vs diameter for fresh catalysts.

Table 2. Experiments with Different Catalyst Composition: Effect of Mg Content (IEA Poplar, 4.9% Moisture, −0.5 mm, N_2 Atmosphere; 600 °C)

	run no.		
	113	121	120
feed rate (g/min)	0.44	0.39	0.45
catalyst	$NiAl_2O_4$	$Ni_3MgAl_8O_{16}$	$NiMgAl_4O_8$
time of reduction with H_2 (min)	30	30	30
WHSV (h^{-1})	0.57	0.47	0.55
run time (min)	61	64.5	60
residence time (s)	0.80	0.87	0.85
yields, wt % mf feed			
gas	93.95	84.09	79.19
water	−3.40	−0.48	−0.68
tar	trace	0.36	0.45
solids (char, coke, soot)	12.01	16.55	21.77
recovery	102.56	100.52	100.73
gas yields, wt % of feed			
H_2	4.72	4.59	4.04
CO	56.17	52.98	46.82
CO_2	25.23	19.87	21.68
CH_4	3.26	2.53	2.67
H_2/CO, vol. ratio	1.16	1.20	1.20
C to gas, wt %	70.8	63.6	59.0
(H_2 + CO), vol %, N_2 free	85.0	87.4	85.1

At this low temperature, small amounts of tar (0.35−0.45%) were produced by the Mg-containing catalysts. Product gas composition did not change significantly as Mg was substituted for Ni, but the activity of the nickel decreased as shown by the lower gas yield and higher

carbon and soot yields. CO and H_2 yields slightly decreased with Ni content. These facts show the influence of $NiAl_2O_4$ as an important carbon−steam gasification catalyst (Arauzo et al., 1994) and suggest that water is more involved in the process than initially supposed.

These results can be interpreted from two different viewpoints, first, according to the probable mechanism of this kind of nickel−alumina catalyst and the influence of Ni content on the activity of the catalyst and, second, with reference to the influence of catalyst structure. As the cracking reactions take place over the catalyst surface, the Mg can act to decrease the surface of the catalyst and therefore reduce the active surface available to the volatiles which are in contact with it. This theory is initially supported by the analyses given in Table 1. Magnesium content clearly modifies the catalyst structure and pore size distribution. Unmodified nickel−alumina catalyst contains a higher fraction of macropores of bigger diameter as shown in Figure 2, where cracking and re-forming of large organic molecules can take place.

Another possible explanation of the lower activity of the Mg-modified catalyst is indicated by the need of higher temperatures of about 850−900 °C for the complete reduction of the catalyst, because small amounts of magnesium appear to drastically influence the reduction rate of the nickel oxide (Rostrup-Nielsen, 1984). In this study a temperature of 750 °C was always used for the reduction step for all catalysts.

As carbon deposition appeared to be the main cause of catalyst deactivation, some tests of catalyst regeneration by carbon combustion were carried out. The catalysts containing magnesium appeared to be more easily restored to their original state than were those with no magnesium. Given the stronger physical structure and potentially greater stability on regeneration, the small reduction in catalyst activity when magnesium was substituted for some of the nickel may well be acceptable.

(b) Effect of Potassium Addition. The four catalysts containing added potassium, intended to serve as a gasification promoter, were evaluated in gasification tests done at 650 °C, with a catalyst activation time of 100 min. In all cases, 50 g of catalyst was the initial charge, run time was 60 min, and nitrogen was used as the fluidizing gas. Results of these tests are given in Table 3, with different catalyst types containing potassium designated by a−d, as defined earlier.

The product compositions obtained indicate small differences in yield among the various catalysts and no clear trends. It was assumed that potassium as a known active gasification catalyst would promote at least the reactions:

$$C + H_2O \leftrightarrow H_2 + CO \quad (1)$$

$$C + CO_2 \leftrightarrow 2CO \quad (2)$$

but this did not seem to be the case although three methods of incorporating the potassium in the catalyst at two levels of concentration were tested. It is possible that the potassium, at our low-temperature gasification conditions, is active primarily in promoting oxygen−carbon reactions and so was largely ineffective in these tests. At the low temperatures and short gas reaction times used in this work, the catalytic effect of potassium on the steam−carbon reaction (1) which is normally observed in conventional gasification at higher temperature was not evident.

Table 3. Experiments with Catalyst Modified with Potassium (IEA Poplar, 4.9% Moisture; −0.5 mm, N_2 Atmosphere; 650 °C)

	run no.				
	123	137	138	140	141
feed rate (g/min)	0.48	0.42	0.38	0.46	0.46
catalyst	$NiAl_2O_4$	a(K)	b(K)	c(K)	d(K)
time of reduction with H_2 (min)	100	100	100	100	100
WHSV (h^{-1})	0.65	0.56	0.49	0.59	0.58
run time (min)	60	60	60	60	60
residence time (s)	0.83	0.80	0.80	0.79	0.79
yields, wt % mf feed					
gas	83.74	86.38	84.42	86.78	88.98
water	−3.36	−3.76	−2.22	−3.64	−3.64
tar	0.00	0.00	0.00	0.00	0.00
solids (char, coke, soot)	16.98	17.40	17.83	16.51	16.72
recovery	97.36	100.02	100.03	99.65	102.06
gas yields, wt % of feed					
H_2	4.36	4.26	5.60	4.29	4.57
CO	58.46	60.80	60.13	60.85	64.42
CO_2	14.46	15.23	12.10	15.56	13.94
CH_4	2.37	2.58	3.00	2.58	2.31
C to gas, wt %	65.1	67.7	66.1	67.9	67.1

Table 4. Experiments with $NiAl_2O_4$ at 650 °C: Effect of the Run Time (IEA Poplar; −0.5 mm, N_2 Atmosphere)

	run no.		
	148	152	212
moisture (wt % feed)	5.8	5.8	6.7
feed rate (g/min)	0.45	0.39	0.30
time of reduction with H_2 (min)	60	60	180
WHSV (h^{-1})	0.58	0.49	0.40
run time (min)	60	213	267
residence time (s)	0.81	0.79	0.80
yields, wt % mf feed			
gas	87.23	85.98	91.64
water	−2.97	−4.67	−6.53
tar	0.00	trace	trace
solids (char, coke, soot)	15.67	14.85	14.16
recovery	99.93	96.16	99.27
gas yields, wt % of feed			
H_2	5.28	4.36	6.58
CO	63.52	61.62	65.20
CO_2	12.13	12.67	10.72
CH_4	2.08	2.34	2.98
H_2/CO, vol. ratio	1.15	0.98	1.31
C to gas, wt %	67.4	67.7	71.5

(c) Catalyst Deactivation. Carbon deposition and catalyst attrition appear to be the most important causes of catalytic deactivation. In order to study these effects, longer runs (152 and 212) were carried out until obvious indications of catalyst deactivation became apparent. Table 4 reports the results obtained. Results are also given for a standard length run (60 min), for comparison (148). For run 152 tar appeared in the cotton filter after about 200 min of operation, showing a deactivation of the catalyst although no important changes in gas composition were observed. Figure 3 shows the changes in gas composition ratios versus time for this long run. It is apparent that it is only after 180 to 200 min of operation that slight changes in product distribution occur. For run 212 no obvious signs of loss of activity were observed after close to 5 h, and only fluidization problems made it difficult to continue the experiment. In run 212, a lower feed to catalyst ratio was used and the catalyst was initially more highly reduced. However, the high CO/H_2 content of the

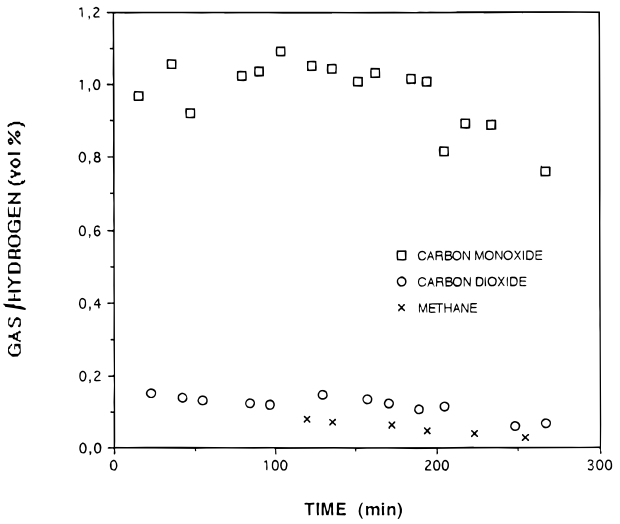

Figure 3. Gas product distribution during catalyst deactivation.

product gas suggests that reduction times of more than 60 min would be adequate even for long runs.

From these results it was concluded that the weight hourly space velocity, WHSV (moisture-free feed rate/ weight of catalyst in the bed after activation), is one of the more important variables, because WHSV determines not only the amount of biomass cracking but also the overall re-forming power of a given catalyst for the molecules produced during the initial step of biomass pyrolysis.

However, in comparison to other runs performed, similar amounts of char + catalyst remained in the fluidized bed and charpot, at the end of these extended runs, so that attrition did not seem to be an important cause of catalyst deactivation. This result also suggested that the carbon buildup on the catalyst surface quickly reached a constant amount. The carbon layer was probably kept constant due to the abrasive action that takes place in a fluidized bed.

Furthermore, a careful examination of all the results on solids production, and comparison to pyrolysis in nitrogen at the same conditions in an uncatalyzed bed, suggests that the "primary pyrolysis char" is produced in about the same yield whether the bed solid is catalytic or not. It is partly on this basis that the proposed mechanism of catalytic biomass gasification is assumed to be an initial thermal pyrolysis followed by reaction on the catalyst surface of the volatile products. If the amount of deposition of the carbon, both primary and secondary, on the catalyst surface soon reaches a constant value, then deactivation most probably results from a decrease in available active surface due to a gradual blocking of the catalyst pores. The outer deposit of carbon on the catalyst surface then does not appear to offer any serious diffusional resistance to passage of the reactants and products to catalytic sites, and in consequence only a slow deactivation is observed.

Finally, another conclusion may be drawn from the results shown in Figure 3 which indicate that all gas−carbon component yields decrease relative to hydrogen after about 200 min, suggesting that cracking reactions are increasing relative to gasification reactions.

(d) Regeneration of the Catalyst. The possibility of maintaining the catalyst activity for long periods of time should make feasible a design for a commercial plant. From results recently obtained and presented in a previous paper (Arauzo et al., 1994), where carbon dioxide, steam, or mixtures of them were used as a gasifying medium, it was shown that it is possible in theory to accomplish a nearly complete gasification of secondary coke or soot which might deposit on the catalyst surface. For noncatalyzed pyrolysis of poplar wood, the normal primary char yield at 650 °C is about 7% of the moisture-free wood fed (Scott et al., 1985). Assuming that catalytic gasification occurs by a process of thermal fast pyrolysis of the wood followed by catalytic cracking and re-forming of the pyrolysis vapors on the catalyst surface, then the primary char yield would be largely unaffected by the presence of the catalyst. At the relatively low temperatures and short reaction times used, little gasification of these discrete primary char particles could be expected. However, secondary carbon deposits on the catalyst surface might be readily gasified by a reactive fluidizing gas. For these reasons, several methods of in situ regeneration of catalysts were tried.

Due to the good results obtained using $NiMgAl_4O_8$ and its adequate physical characteristics for a fluidized-bed process, combined with a good activity level, this catalyst was selected for performing tests to identify possible regeneration and design strategies. Two different alternatives were tried: (i) regeneration of the catalyst once the run was concluded and (ii) regeneration of the catalyst during the run by using different gasifying mediums.

As a test of the first alternative, after a run was completed, a slow combustion, "in situ" at 500 °C, of the carbon deposited upon the catalyst was done. It was noticed that small amounts of H_2 and CO were evolved during the heating period up to 500 °C, using exclusively nitrogen as a fluidizing gas. This effect may be due to a small adsorption of these species by the catalyst. After this slow oxidation, the bed appeared to be completely clean of coke and the catalyst displayed the original green color.

Following this procedure an experiment, run 158, was carried out with a catalyst regenerated in this way, previously used in run 157. From the results (Table 5) obtained it appears probable that a deactivation of the catalyst did not take place due to the regeneration. The activity of the catalyst seemed to be similar to that of the fresh material, and it is most likely that loss of catalyst (by attrition or by catalyst blown into the charpot) produced the observed changes in the product distribution and gas composition.

The second regeneration possibility was based on the effects observed when reactive gasification media such as CO_2 or steam were used and where a good level of oxidation of the deposited carbon was achieved. The first test (Table 5, run 163) was done by introducing a small amount of oxygen (0.25 L/min of air). The amount of oxygen was calculated according to the amount of coke deposited over the surface of the catalyst during run 157. A low sand/catalyst ratio was chosen in order to emphasize as much as possible the effect of coke gasification.

The most representative values are the percentages of carbon reacting to gas and coke. Carbon to coke was somewhat smaller and carbon to gas slightly higher than run 157, which means an effective gasification of the secondary char (coke) was taking place, but not at the expected rate. In consequence, the coke gasification rate was probably slower than the formation at 650 °C. The result suggests that classical configuration of two parallel fluidized-bed reactors, the first one for the catalytic gasification process and the second one for

Table 5. Experiments with $NiMgAl_4O_8$ at 650 °C: Effect of Catalyst Regeneration (IEA Poplar, 5.8% Moisture, −0.5 mm)

	run no.		
	157	158	163
feed rate (g/min)	0.51	0.51	0.53
time of reduction with H_2 (min)	60	60	60
ratio sand/catalyst (vol)	3/1	ND[a]	3/1
ratio sand/catalyst in run (wt)	6	ND[a]	6
WHSV (h^{-1})	2.63	ND[a]	2.74
atmosphere	N_2	N_2	N_2/O_2
run time (min)	60	60	60
residence time (s)	0.86	0.79	0.78
yields, wt % mf feed			
gas	75.07	69.14	84.76
water	−1.27	−1.02	−4.44
tar	10.68	18.79	12.98
solids (char, coke, soot)	13.97	11.98	13.37
recovery	98.45	98.89	115.55
gas yields, wt % of feed			
H_2	3.33	2.76	2.45
CO	52.92	46.29	38.18
CO_2	10.16	10.30	30.76
CH_4	2.28	1.97	2.92
C_2H_4	0.53	0.77	1.12
C_2H_6	0.13	0.18	0.32
C_3H_6	0.25	0.32	0.60
oxygen comp.	1.10	2.53	3.47
H_2/CO, vol. ratio	0.87	0.83	0.89
C to gas, wt %	61.4	58.4	67.4
C to coke, wt %	19.0	19.2	16.8

[a] Not determined.

catalyst regeneration (combustion of the coke), would be an adequate technology if coke deposition cannot be avoided.

According to studies carried out by Ashcroft et al. (1991), nickel−alumina catalysts showed no carbon deposition when oxidation of methane using carbon dioxide was taking place. Pursuant to this possibility, another run (run 166) with a mixture of $N_2/CO_2/O_2$ as the fluidizing gas in a ratio of 46.5/49/4.5 (vol %) was carried out at 700 °C in order to get a qualitative idea of how the reversible reactions involved in the process may be affected by different variables. The sand/catalyst volumetric ratio was 7/1. Oxygen was only introduced after 2 min of time on stream. The other operating variables were similar to those of run 163.

It was experimentally observed that the small amount of oxygen produced an effective gasification of coke, increased the temperature of the reactor, and reduced the smoke that visually usually appeared in the condensers when a deactivated catalyst was used or simulated.

If wood is not fed, coke gasification proceeds according to reaction (2). At the same time the water−gas shift reaction is moved in the same direction, that is, to the right side as shown below:

$$CO + H_2O \leftrightarrow CO_2 + H_2 \qquad (3)$$

The overall result it that an indirect steam gasification of the coke is taking place, reaction (1).

Methane content would remain constant at this temperature (less than 700 °C) independently of which gas mixture is used for the coke gasification.

The final result of this test was that only 5.0% of mf feed as coke, char, or soot remained after 75 min of the run, compared to normal yields of 13−18%. Also, the 5% char yield was very likely entirely primary pyrolysis char.

(e) Simulation of the Catalyst Deactivation. Because the deactivation process was a very slow process and fluid dynamic problems did not allow operation for long periods of time, it was necessary to develop a procedure that would allow us to evaluate the lifetime of the catalyst by data from shorter experiments, in our case, runs of 1 h. The procedure was to replace a part of the catalyst by sand, but always keeping constant the depth of the bed (10 cm) in order to maintain the same fluid dynamic conditions. Sand/catalyst volumetric ratios of 0/1, 1/1, 3/1, and 7/1 were tested at two temperatures, 600 and 650 °C. The assumption was that a reduced amount of relatively fresh catalyst could be an indicator of a proportionate drop in activity of a bed of catalyst with time on stream. Results are shown in Table 6.

A comparison at the two temperatures shows similar trends; that is, as the amount of catalyst present in the bed decreased, a lower percentage of gas was produced, less solid remained on the surface of the catalyst, and a higher amount of tar was collected in the condenser, which indicated that the surface coke was generated during the cracking of the tar. Data given in Table 6 on the percentage of feed carbon converted to gas and to coke corroborate this conclusion, so a smaller amount of catalyst represents less cracking activity from it, and, in consequence, less coke production can be expected, as the data show.

At the higher temperature, the percentage of gas evolved increased at the expense of the amount of tar condensed, so the yield of solid residue was more or less constant for a given sand/catalyst ratio. The quality or composition of the gas changed also as the feed/catalyst ratio changed; for instance, one main result was a higher percentage of C_2, C_3, and C_4 as the sand/catalyst ratio increased.

These results also corroborate the idea that the WHSV is one of the major variables determining the cracking and re-forming power of a given catalyst.

Kinetics of Formation of the Tar. The period during which no tar evolution was observed changed depending on the sand/catalyst ratio, so from visual observation the time at which tar appeared in the condensers increased as the sand/catalyst volumetric ratio decreased.

During runs shown in Table 6, a constant CO/CO_2 composition ratio was observed, not dependent on tar evolution rate, and only after 35 min in run 159 at 650 °C and after 20 min in run 165 at 600 °C was a lower CO/CO_2 ratio observed. Apparently, the gas achieved equilibrium composition faster than the cracking process was taking place.

It may be possible to represent the deactivation kinetics of this process by a simple first-order rate equation, which has often been found to be empirically adequate in other biomass gasification or pyrolysis investigations.

$$-dM/dX = kM \qquad (1)$$

where M = fractional yield of tar (weight percent of mf feed) and k = kinetic constant of cracking and re-forming reactions.

$$X = \frac{W_{catalyst}}{W_{sand} + W_{catalyst}} \qquad (2)$$

where $X = 0$ for sand only and $X = 1$ for catalyst only and W = weight of material.

Table 6. Experiments with $NiMgAl_4O_8$ at Different Sand/Catalyst Ratios (IEA Poplar, −0.5 mm, N_2 Atmosphere)

	run no.							
	120[a]	164	161	165	153	156	157	159
moisture (wt % feed)	4.9	5.8	5.8	5.8	5.8	5.8	5.8	5.8
temperature (°C)	600	600	600	600	650	650	650	650
feed rate (g/min)	0.45	0.50	0.55	0.52	0.41	0.52	0.51	0.53
time of reduction with H_2 (min)	30	60	60	60	60	60	60	60
WHSV (h^{-1})	0.55	1.25	2.76	5.80	0.50	1.34	2.63	5.80
ratio sand/catalyst (vol)	0/1	1/1	3/1	7/1	0/1	1/1	3/1	7/1
ratio sand/catatlyst in run (wt)	0	2.04	5.89	15.24	0	2.00	6.05	14.95
run time (min)	60	60	60	60	60	60	60	60
residence time (s)	0.85	0.85	0.87	0.90	0.84	0.84	0.86	0.84
yields, wt % mf feed								
gas	79.19	77.52	62.25	48.50	88.87	83.13	75.07	67.62
water	−0.68	−1.74	−0.78	−2.60	−2.93	−2.81	−1.27	−0.63
tar	0.45	5.70	23.40	41.50	trace	2.66	10.68	22.43
solids (char, coke, soot)	21.77	17.04	11.42	11.43	15.04	17.44	13.97	10.50
recovery	100.73	98.52	96.29	98.83	100.98	100.42	98.45	99.92
gas yields, wt % of feed								
H_2	4.04	3.03	2.48	1.85	4.95	4.13	3.33	2.22
CO	46.82	47.46	35.54	25.92	64.04	59.13	52.92	41.67
CO_2	21.68	17.64	15.33	11.03	13.13	11.61	10.16	11.28
CH_4	2.67	3.96	2.73	2.25	1.75	2.70	2.28	2.75
C_2H_4	nd[b]	0.18	0.45	0.73	nd[b]	0.19	0.53	1.07
C_2H_6	nd[b]	0.05	0.12	0.26	nd[b]	0.05	0.13	0.29
C_3H_6	nd[b]	0.09	0.24	0.37	nd[b]	0.08	0.25	0.52
oxygen comp.	nd[b]	0.65	1.76	3.56	nd[b]	0.40	1.10	3.89
H_2/CO, vol. ratio	1.20	0.88	0.95	0.99	1.07	0.97	0.87	0.74
C to gas, wt %	59.0	61.6	50.5	42.0	69.0	66.6	61.4	59.4
C to coke, wt %	ND[c]	19.8	19.3	15.7	ND[c]	ND[c]	19.0	11.9

[a] This run was done with catalyst from a different batch. [b] Not detcted. [c] Not determined.

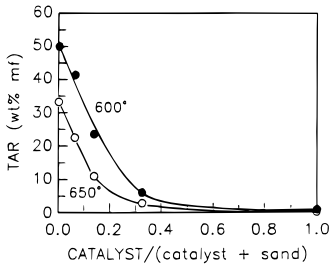

Figure 4. Experimental simulation of deactivation kinetics of $NiMgAl_4O_8$ catalyst.

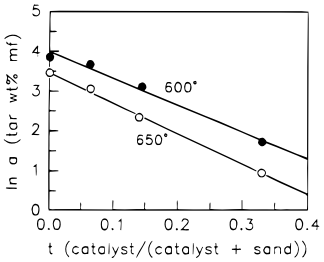

Figure 5. Plot for first-order behavior of deactivation kinetics.

Equation 1 may be considered similar to the simple classical deactivation equation:

$$-\mathrm{d}a/\mathrm{d}t = ka \tag{3}$$

where a represents the activity of the catalyst. This activity is measured by the tar production, and the time is simulated by different concentrations of the catalyst in the bed so $X = 1$ (pure catalyst) corresponds to run time 0 and $X = 0$ (pure sand) to infinitely long time. This assumes that the characteristic time scale for catalyst deactivation is much longer than the duration of a run. The different X values used represent different stages of catalyst activity, for example, catalyst after 1, 2, 3, 4, 5, ... h of operation. The real time should be determined experimentally in a plant with recirculation.

From noncatalytic experiments tar values were determined: $M = 50.1$ at 600 °C and $M = 33.2$ at 650 °C (Scott et al., 1990). The experimental curves obtained are shown in Figure 4.

Equation 1 can be written as:

$$\ln M = \ln M_0 - kX \tag{4}$$

where M_0 is the tar production with no catalyst, i.e., at $X = 0$. Equation 3 can also be written as:

$$\ln a = \ln a_0 - kt \tag{5}$$

If $X = 1$ is equated to a zero time, representing fresh catalyst, and $X = 0$ to an infinitely long run time with completely deactivated catalyst, then the rate expression in the form of eq 5 can be used as shown in Figure 5.

From Figure 5, eqs 4 and 5 take values of:

$$600\ °\mathrm{C} \qquad \ln a = 4.0478 - 6.1823t \tag{6}$$

$$650\ °\mathrm{C} \qquad \ln a = 3.5233 - 7.7582t \tag{7}$$

where t is the fractional time to complete deactivation ($t = 1$; and for fresh catalyst, $t = 0$).

Similar low slopes are obtained at both temperatures, showing that the catalytic process involves only a low activation energy, estimated from eqs 6 and 7 as about 17 500 J/mol. Therefore, the nickel−magnesium−alumina catalyst appears to be working satisfactorily, but more catalyst development would be desirable in order to avoid the loss of activity caused by the incorporation of Mg in the crystal lattice.

Tar Nature. Tar analyses were made by GC−MS; Figure 6 shows a typical report. The nature of these tars is different than those reported by Mudge et al. (1987) in studies conducted at Pacific Northwest Laboratory. In particular, the tar produced in this work appears to best be described as unconverted primary pyrolysis tar rather than the more intractable secondary tars consisting of polynuclear aromatic hydrocarbons,

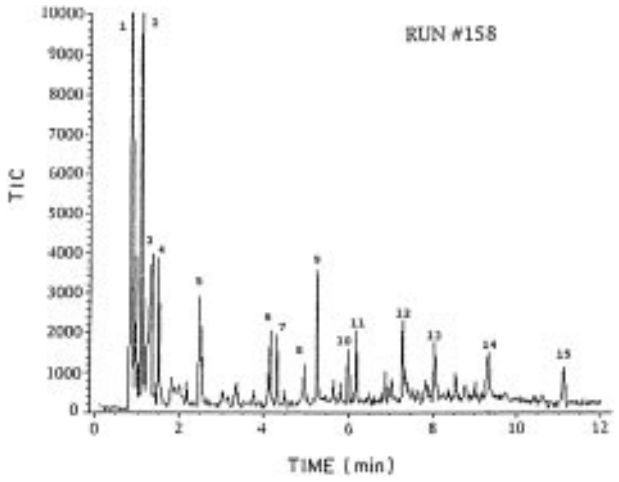

Figure 6. Total ion count in GC−MS of tar from run 158: 1, 3-oxoethyl ester butanoic acid; 2, hydroxyacetaldehyde; 4, 1-hydroxy 2-propanone; 5, 2,3-pentanedione; 9, phenol; 10, 2-methylphenol; 11, 3-methylphenol; 12, 1,2-benzenediol; 13, 3-methyl-1,2-benzenediol; 14, levoglucosan; 15, pentadecanoic acid.

which have been reported as the normal product of high-temperature gasification (Mudge et al., 1987).

Discussion

Both the results presented here as well as those discussed in our previous paper (Arauzo et al., 1994) suggest that the composition of the product gas is close to equilibrium. In consequence, it should be possible to establish a composition of the gasifying medium in order to obtain the most desirable final gas product. This fact also leads us to a concept for the design of a continuous plant where a recirculation process would be taking place and where the inlet gas composition could be changed according to needs. A conceptual scheme of such a plant is presented in Figure 7. Except for the air inlet before the gas turbine, no other flow or heat addition would be necessary, as the heat required for gasification would be supplied by combustion of the char and coke in the preheater. Carbon dioxide is assumed to be the fluidizing gas, supplied by a CO_2 absorption−stripping system. A gasification system of this type could ensure that a high percentage of the carbon in the feed is utilized in the desired form, that is, as carbon monoxide, while maintaining catalyst activity for longer periods.

A preliminary theoretical study of the operation of this plant has been carried out by development of computer programs based on thermodynamic equilibrium calculations (Eriksson, 1971; Uchida, 1987). As a first approach, three possibilities have been simulated at operating conditions similar to the experiments performed. The results of the computer program are presented in Figures 8 and 9. The initial operating conditions selected were:

nitrogen flow (m^3(STP)/h)	183
temperature (°C)	650
pressure (atm)	1
biomass feed rate (kg/h)	35
moisture content (%)	4.92

For option A an initial steam flow of 10.9 m^3(STP)/h was used, and for the next hour the water (steam), methane, and carbon dioxide produced were introduced in the program as feed for the following hour and so on. After 4−5 h (four runs of the program), the results

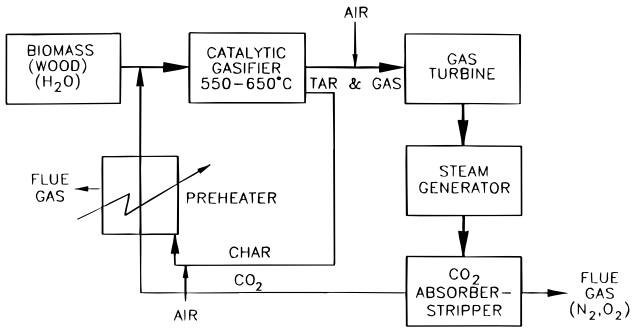

Figure 7. Conceptual catalytic pyrogasification process for biomass.

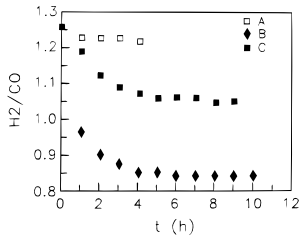

Figure 8. Predicted performance of conceptual pyrogasification process H_2/CO ratio: (A) initial steam and then recycling of CO_2, CH_4, and H_2O products; (B) recycling of CO_2, CH_4, and H_2O products; (C) constant steam addition plus recycling of CO_2, CH_4, and H_2O products.

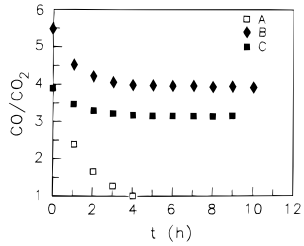

Figure 9. Predicted performance of conceptual pyrogasification process CO/CO_2 ratio: A−C as for Figure 8.

were steady and our hypothetical plant would operate in steady state.

For option B no water was initially introduced, but similar to option A, the H_2O, CH_4, and CO_2 produced were recirculated from one run to the next run, etc. After 5 h the plant would operate in a steady state.

Option C was similar to A but the steam flow was kept constant at 11 m^3(STP)/h, independent of steam produced during processing. Results similar to option B can be observed for the CO/CO_2 ratio, but option C gives a higher H_2/CO ratio than option B, as expected. Option B (no extra H_2O added) gives the highest CO/CO_2 ratio and the lowest H_2/CO ratio, both of which would be desirable for a system to produce a maximum amount of CO from the biomass fed.

Conclusions

(1) Partial replacement of nickel by magnesium improved the strength of the catalyst but gave a lower gas yield and a significant increase in char production.

(2) Additions of potassium into a nickel aluminate stoichiometric catalyst did not improve the catalyst characteristics for char gasification.

(3) Temperature and feed rate/catalyst ratio are the most important variables that determine the final product distribution and lifetime of the catalyst.

(4) The deactivation of $NiAl_2O_4$ and $NiMgAl_4O_8$ catalysts is a slow process. $NiMgAl_4O_8$ deactivation can

be modeled as a first-order process which involves a low activation energy of 17 500 J/mol. An easy regeneration of both catalysts can be done by either of two different procedures and without appreciable activity decay.

(5) After some deactivation of the catalyst has taken place, tar production appears, and analysis of this tar indicates that it is an unconverted primary pyrolysis tar.

Acknowledgment

The authors are indebted to the Alternative Energy Division, CAMMET, Energy, Mines and Resources Canada, and to the Natural Sciences and Engineering Research Council of Canada for financial support of this work. J.A. thanks Dirección General de Investigación Científica y Técnica (M.E.C. Spain) and Instituto Aragones de Fomento (Spain) for grants awarded. We also express our thanks to Dipartamento de Ingeniería Química y T.M.A., University of Zaragoza, Spain, for assistance with measurements of the physical characteristics of the catalysts. The assistance of Piotr Majerski in solving equipment problems and his help with analytical work are also gratefully acknowledged.

Literature Cited

Arauzo, J.; Radlein, D.; Piskorz, J.; Scott, D. S. A New Catalyst for the Catalytic Gasification of Biomass. *Energy Fuels* **1994**, *8*, 1192−1196.

Ashcroft, A. T.; Cheetham, A. K.; Green, M. L. H.; Vernon, P. D. F. Partial Oxidation of Methane to Synthesis Gas Using Carbon Dioxide. *Lett. Nature* **1991**, *325*, 225−226.

Beenackers, A. A. C. M.; Bridgwater, A. V. Gasification and Pyrolysis of Biomass in Europe. *Pyrolysis and Gasification*; Ferrero, G. L., et al., Eds.; Elsevier Applied Science Publishers: London, 1989; pp 129−157.

Bridgwater, A. V.; Double, J. M. A Strategic Assessment of Liquid Fuels from Biomass. *Research in Thermochemical Biomass Conversion*; Bridgwater, A. V., Kuester, J. L., Eds; Elsevier Applied Science Publishers: London, 1988; pp 98−110.

Eriksson, G. Thermodynamic Studies of High Temperature Equilibria. *Acta Chem. Scand.* **1971**, *25* (7), 2651−2658.

Garg, M.; Piskorz, J.; Scott, D. S.; Radlein, D. The Hydrogasification of Wood. *Ind. Eng. Chem. Res.* **1988**, *27*, 256−264.

Koryabkina, N. A.; Ismagilov, Z. R.; Shkabina, R. A.; Moroz, E. M.; Ushakov, V. A. Influence of the Method of Alumina Modification on Formation of Low Temperature Solid Solutions in Magnesia−Alumina Systems. *Appl. Catal.* **1991**, *72*, 63−69.

Mudge, L. K.; Baker, E. G.; Brown, M. D.; Wilcox, W. A. Bench Scale Studies on Gasification of Biomass in the Presence of Catalysts. Final report, Pacific Northwest Laboratory, Battelle Memorial Institute, Contract DE-AC0676RLO-1830, Richland, WA, Nov 1987; PNL-5699.

Ovsyannikova, I. A.; Gold'denberg, G. I.; Koryabkina, N. A.; Shkrabina, R. A.; Ismagilov, Z. R.; Study of Structural and Mechanical Properties of Granulated Alumina Supports Using X-Ray Microprobes. *Appl. Catal.* **1989**, *55*, 75−80.

Rostrup-Nielsen, J. R. Catalytic Steam Reforming. *Catalysis Sicence and Technology*; Andersen, J. R., Bourdart, M., Eds.; Springer: Berlin, 1984; Vol. 5, pp 1.

Scott, D. S. Production of Hydrocarbons from Biomass Using the WFPP. Final Report, Contract 061SZ-232883-8-6067, Renewable Energy Division, Energy, Mines & Resources Canada, Ottawa, Canada, 1990.

Scott, D. S.; Piskorz, J. The flash Pyrolysis of Aspen−Poplar Wood. *Can. J. Chem. Eng.* **1982**, *60*, 666−674.

Scott, D. S.; Piskorz, J.; Radlein, D. Liquid Products from the Continuous Flash Pyrolysis of Biomass. *Ind. Eng. Chem. Process Des. Dev.* **1985**, *24*, 581−588.

Uchida, M. MPEC2: A Code for Multi-Phase Chemical Equilibria. *Comput. Chem.* **1987**, *11* (1), 19−24.

Received for review April 5, 1995
Revised manuscript received August 20, 1996
Accepted September 30, 1996[⊗]

[⊗] Abstract published in *Advance ACS Abstracts,* November 1, 1996.